

# High-pressure optical and vibrational properties of Ga<sub>2</sub>O<sub>3</sub> nanocrystals

Alberto del Moral Cejudo

*Dr. Jordi Ibáñez, Institute of Earth Sciences Jaume Almera (ICTJA-CSIC), Lluís Solé i Sabarís s/n, 08028 Barcelona, Catalonia, Spain*

*Dr. Sergi Hernández, MIND-IN<sup>2</sup>UB, Department of Electronics, University of Barcelona, Martí i Franquès 1, 08028 Barcelona, Catalonia, Spain*

**Abstract**—In this project the optical and vibrational properties of monoclinic gallium oxide ( $\beta$ -Ga<sub>2</sub>O<sub>3</sub>) nanocrystals (NCs) are studied by Raman scattering spectroscopy under high-hydrostatic pressure conditions, from ambient pressure up to 21.6 GPa. Phonon pressure coefficients and Grüneisen parameters are obtained for different optical phonon modes of nanocrystalline  $\beta$ -Ga<sub>2</sub>O<sub>3</sub>. In the first part of the work, the investigated material is characterized by means of different techniques like X-ray diffraction (XRD), scanning electron microscopy (SEM) and Raman scattering. While XRD and SEM confirm the nanocrystalline nature of the investigated sample, from the Raman spectra we are able to properly identify the Raman-active modes of  $\beta$ -Ga<sub>2</sub>O<sub>3</sub> at ambient pressure. By monitoring their peak position at different pressures, phonon pressure coefficients for several of the optical Raman-active modes of  $\beta$ -Ga<sub>2</sub>O<sub>3</sub> have been successfully determined, with values significantly lower than those reported in previous works for bulk  $\beta$ -Ga<sub>2</sub>O<sub>3</sub>. This suggests that the compressibility of the NCs could be reduced with respect to the bulk material. In order to test the validity of the experimental data, density functional theory calculations of the structural properties of bulk  $\beta$ -Ga<sub>2</sub>O<sub>3</sub> have also been performed as a function of pressure. From the *ab initio* calculations we obtain a bulk modulus of  $160.7 \pm 5.0$  GPa for bulk  $\beta$ -Ga<sub>2</sub>O<sub>3</sub>, which is comparable, and even lower, than that measured in previous works for bulk material by means of synchrotron XRD as a function of pressure ( $\sim 200$  GPa). Our theoretical results thus confirm that the lower compressibility of the  $\beta$ -Ga<sub>2</sub>O<sub>3</sub> NCs studied in this work may be a consequence of the nanocrystalline nature of the investigated material. The possible physical mechanisms giving rise to this observation are discussed in terms of similar results reported in the literature. It is concluded that more work dealing with the high-pressure structural and vibrational properties of  $\beta$ -Ga<sub>2</sub>O<sub>3</sub> samples of different origin (i.e., bulk vs. NCs, and doped vs. undoped material) should be performed in order to fully understand the origin of the lower compressibility displayed by the nanocrystalline  $\beta$ -Ga<sub>2</sub>O<sub>3</sub> sample studied in this work.

**Index Terms**—5. Nanostructured materials; Raman-scattering spectroscopy, high-hydrostatic pressure, Density Functional Theory, gallium oxide, nanocrystals.

## I. INTRODUCTION

NANOSTRUCTURED materials are widely studied as an alternative to conventional bulk materials since relevant phenomena have been observed, such as the tuning of their optical and electronic properties by controlling the size.

During the last decades there have been numerous works on nanostructured semiconductors focused in the study of their structural and optical properties for different sizes or geometries. In particular, nanocrystals (NCs) present a broad variety of modified properties over bulk material, like a confinement of the electronics states, which leads to discretized energetic states in the confinement direction, with a band-gap energy that increases with decreasing the nanocrystal size.

Raman spectroscopy has long been recognised as a useful technique for chemical analysis of both stable and transient species [1]. Moreover, it is used to characterize materials and determine their crystallographic or amorphous structure, orientation, strain and composition, as well as to investigate optical and vibrational properties [2]. In this framework, Raman scattering has proved itself as a potential tool to characterize nanostructured semiconductors [3].

High-pressure Raman measurements provide a useful benchmark to test the validity of existing theoretical models, thereby investigating the fundamental properties of semiconductors and their lattice-dynamical properties, such as vibrational frequencies, dielectric constants and even the optical gaps [4]–[9]. Pressure-induced frequency shifts of the Raman bands strongly depend on the nature (optical or acoustic) and number of phonons involved in the Raman-scattering processes. Thus, the application of high hydrostatic pressures to study the vibrational modes can allow one to identify unknown Raman peaks. More importantly, it may provide further information about thermodynamic properties of the crystal, as for instance the Grüneisen parameters.

The pressure behaviour of nanostructured materials may differ from that of bulk or thin films due to, among others, surface effects, matrix-induced strain, bending, softening or stiffening effects [4], [9]. For instance, silicon nanocrystals (SiNCs) embedded in a SiO<sub>2</sub> matrix were studied by Ibáñez *et al.* [4] with the aim of exploring the origin of the optical emission of the active layers. They reported phonon pressure coefficients sizably larger than those of bulk Si, indicating that the NCs are subject to a strong pressure amplification effect as a consequence of a matrix-induced strain effect. Thus, in this case there is a pressure amplification effect on the NCs as a consequence of the larger compressibility of the SiO<sub>2</sub> matrix in relation to the SiNCs.

In the last decade gallium oxide (Ga<sub>2</sub>O<sub>3</sub>) has attracted considerable attention, as it is a wide band-gap semiconductor that has been considered for numerous applications: as catalyst for chemical reactions, as a new phosphor host material for emissive display applications including thin-film field emission and electroluminescent displays [10], as main element for gas sensors, for transparent conductive coatings or dielectric thin films, as magnetic memory material and as a promising material for power and high voltage electronic devices [11].

Among all the Ga<sub>2</sub>O<sub>3</sub> polymorphs, the  $\beta$ -Ga<sub>2</sub>O<sub>3</sub> is the most common and the only stable form through the whole temperature range till the melting point [11]. Different polymorphic forms present different physical properties, being the band-gap energy of the most relevant. This  $\beta$ -form presents several interesting properties, such as its wide band gap energy of  $\sim 4.9$  eV, high transparency within the visible range and high breakdown voltage [12]. This form corresponds to a C-centered monoclinic cell with space group C2/m (see the inset of Fig. 2 for a sketch of the unit cell, which has four formula units). As it happens to other polymorphs, there is not yet much available data about  $\beta$ -Ga<sub>2</sub>O<sub>3</sub> since its structural characterization has been hampered by its typically poor crystalline nature. However, it has been observed a poor thermal conductivity strongly dependant on the different crystal direction [10]–[12].

In spite of the increasing interest that this compound has gained over the last few years, the high pressure behaviour of  $\beta$ -Ga<sub>2</sub>O<sub>3</sub> has not received much attention so far. In Ref. [13], Machon *et al.* used synchrotron X-ray diffraction and Raman spectroscopy, and observed a phase transformation the monoclinic  $\beta$ -Ga<sub>2</sub>O<sub>3</sub> to a rhombohedral  $\alpha$ -Ga<sub>2</sub>O<sub>3</sub> at a pressure above 20-22 GPa. However, Lipinska-Kalita *et al.* [14] observed that the same transition began at 6.5-7 GPa. Pressures up to 64.9 GPa were reached by Wang *et al.* [15] at ambient temperature, again observing this phase transition that began at 13.6-16.4 GPa and extended up to 39.2 GPa, with only  $\alpha$ -form at the highest pressure. Other intervals for the transition have been found in diverse works [16]–[17].

The significance of the pressure-induced phase transformations among Ga<sub>2</sub>O<sub>3</sub> polymorphs relies on the determination of stable and metastable phase relations between different crystalline modifications, and this is a fundamental issue in the mechanical stresses present during the synthesis processes.

In this project we investigate the optical properties of monoclinic gallium oxide nanocrystals ( $\beta$ -Ga<sub>2</sub>O<sub>3</sub> NCs) as a function of high hydrostatic pressure, with the aim of obtaining the phonon pressure coefficients and Grüneisen parameters of the NCs and, more importantly, to determine the influence of the nanocrystalline nature of the studied samples on their compressibility. For this purpose, Raman scattering measurements of  $\beta$ -Ga<sub>2</sub>O<sub>3</sub> NCs have been performed as a function of pressure, up to 21.6 GPa, by using the diamond anvil cell technique. We compare the experimental pressure coefficients and Grüneisen parameters with those reported in the literature for bulk material, and we discuss these results in terms of *ab initio* calculations of the structural properties of bulk  $\beta$ -Ga<sub>2</sub>O<sub>3</sub>.

## II. EXPERIMENTAL DETAILS

The sample employed for this study is a commercially available  $\beta$ -Ga<sub>2</sub>O<sub>3</sub> nanopowder with  $\geq 99.99\%$  trace metal basis, provided by Sigma-Aldrich. Prior to the high-pressure study, several experiments were performed to characterize the  $\beta$ -Ga<sub>2</sub>O<sub>3</sub> sample. With the aim of confirming the nanostructure character of the  $\beta$ -Ga<sub>2</sub>O<sub>3</sub> material, scanning electron microscopy (SEM) images and X-ray diffraction (XRD) patterns were acquired.

SEM images were acquired in a JSM-7100F Field Emission Scanning Electron Microscope operated at 20 kV. Figure 1 shows the  $\beta$ -Ga<sub>2</sub>O<sub>3</sub> sample morphology as aggregates (Fig. 1a) of structures approximately 1.9  $\mu\text{m}$  long and 0.47  $\mu\text{m}$  wide (see Fig. 1b), formed from agglomerations of crystallites that range from tens to hundreds of nanometers (see Fig. 1c). In spite of the nanocrystals agglomerations, the sizes obtained are in agreement with available literature about  $\beta$ -Ga<sub>2</sub>O<sub>3</sub> [12].

The XRD measurements were carried out with a Bruker D8-A-25 diffractometer, equipped with a Cu X-ray source (Cu K $\alpha$  radiation,  $\lambda = 1.5406$  Å) and a LynxEye position sensitive detector (PSD). The scans were acquired between 3 and 70° in 2 $\theta$  at 0.015° steps. Phase identification was performed with the DIFFRAC.EVA software together with the Powder Diffraction File PDF-2 and the Crystallography Open Database (COD). Full-pattern analyses were carried out with the Rietveld method [18] by using the TOPAS 4.2 program from Bruker. Pseudo-Voigt peak shape functions were employed to calculate the theoretical diffraction peaks. From the Rietveld analysis, the lattice parameters of  $\beta$ -Ga<sub>2</sub>O<sub>3</sub> were

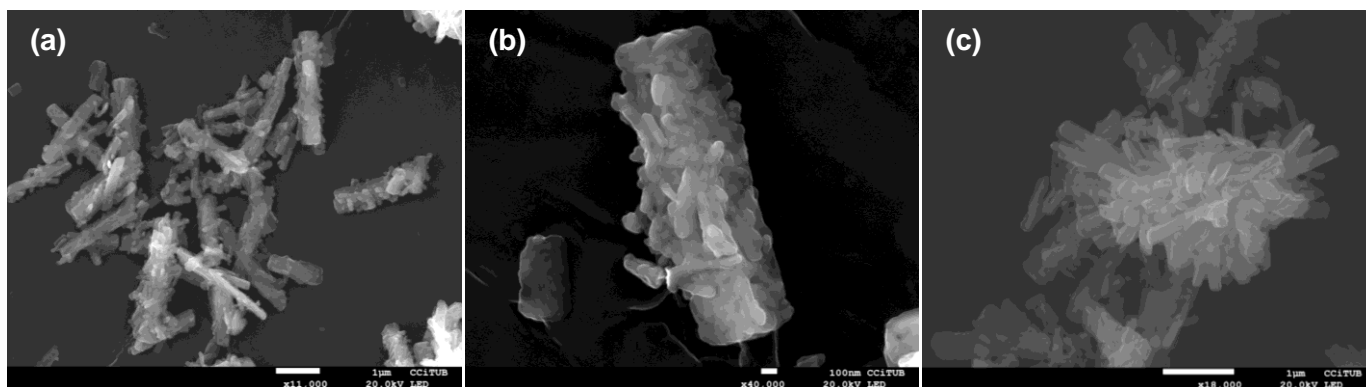


Fig. 1. SEM images of the  $\beta$ -Ga<sub>2</sub>O<sub>3</sub> NCs agglomerated in form of nanopowder; commercial sample with chemical purity 99.99% and provided by Sigma-Aldrich

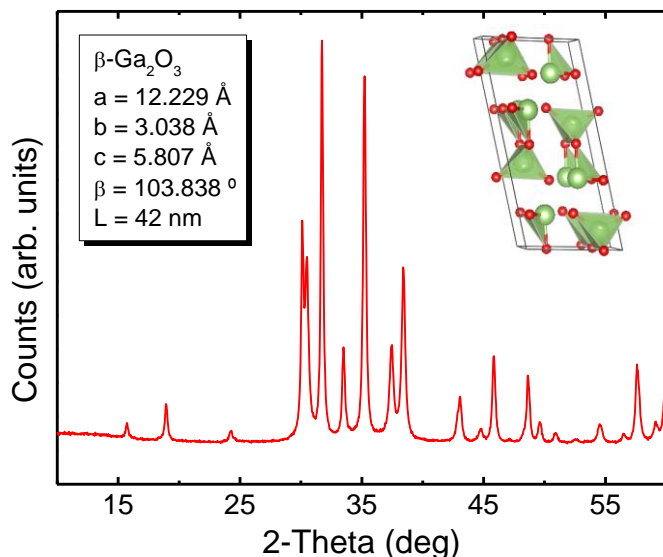


Fig. 2. XRD spectra for the  $\beta$ -Ga<sub>2</sub>O<sub>3</sub> at room temperature and atmospheric pressure. Representation of the crystalline structure of the  $\beta$ -Ga<sub>2</sub>O<sub>3</sub> cell, its coordinate parameters and the nanocrystals average size of 42 nm.

refined and the size of the NCs was estimated by considering a Lorentzian convolution to account for the broadening of the XRD reflections. The XRD pattern (see Fig. 2) confirms the  $\beta$ -Ga<sub>2</sub>O<sub>3</sub> phase, with no traces of the  $\alpha$  phase. The diffraction peaks can be readily indexed as monoclinic crystal structure, C2/m space group, and the refined lattice parameters are  $a$  (Å) = 12.229,  $b$  (Å) = 3.038,  $c$  (Å) = 5.807 and  $\beta$  = 103.84°. These values are in good agreement with previously published data [19]–[20]. From the Rietveld refinement an average crystal size of 42 nm is found. According to a less involved estimate of the nanocrystalline size using the Scherrer model, a value equal to 36 nm is obtained. Both XRD results are in agreement with the values extracted from the SEM images, thus confirming the nanostructured nature of the studied material.

Raman-scattering measurements were performed at ambient pressure conditions and under high hydrostatic pressure. The monochromatic light source used for excitation during Raman-scattering measurements was a 532-nm solid-state laser (Nd:YAG), with a power of 1.5 mW on the sample. The spectrum was obtained by an optical microscope coupled to a Horiba Jobin Yvon LabRAM spectrometer. The scattered light was collected by a charge-coupled device (CDD) detector cooled down by a Peltier device. In this case, the spectrum was corrected in frequency using a silicon spectra reference.

High-hydrostatic pressure was achieved by using a diamond anvil cell (DAC) [21]–[22] (see Fig. 3), consisting in a gasketed membrane-type with two opposing diamonds with a culet of 400  $\mu$ m. Uniaxial pressure was applied to the anvils using pneumatic pressure applied to the membrane; the gas used in this case was helium, with the aim of preventing metal corrosion. The nanopowder was loaded between both diamonds after preindentation and micro-drilling of the gasket. By compressing the pistons of both diamonds, pressures up to 21 GPa were achieved. The uniaxial pressure supplied by the piston is transferred into hydrostatic pressure through the

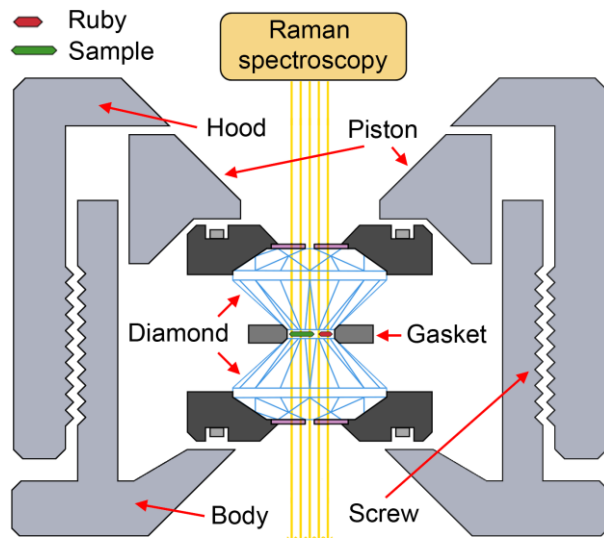


Fig. 3. Schematic representation of the membrane-type DAC, composed of three independent parts: the piston, the body and the hood. Note that inside the gasketed membrane the sample and the ruby are located.

pressure transmitting medium present into the DAC, in this case silicone oil. For the applied pressure measurements the ruby fluorescence method was used [23], and thus a few ruby chips had to be previously loaded together with the sample.

### III. RESULTS

Raman scattering measurements of the  $\beta$ -Ga<sub>2</sub>O<sub>3</sub> NCs studied in this work were first performed in absence of any pressure transmitting medium, at ambient temperature and pressure conditions (i.e., outside the DAC).  $\beta$ -Ga<sub>2</sub>O<sub>3</sub> has 20 atoms in the unit cell but, since it is C-centered, it contains the primitive cell twice. Thus, up to  $3 \times 10 = 30$  normal modes of vibration at the  $\Gamma$  point are expected for this compound. From symmetry analysis, using the notation for the different irreducible representations from group theory, the total reducible representation for the zone-center ( $\Gamma$  point) phonons of this compound is  $\Gamma = 10A_g + 5A_u + 5B_g + 10B_u$ . Three of these modes correspond to acoustic phonons ( $\Gamma_{ac} = A_u + 2B_u$ ), and 27 to optical modes. Among these, 12 modes are IR-active and Raman-inactive, since the crystal is centrosymmetric, while 15 modes correspond to the Raman-active (IR-inactive) phonons. The irreducible representation for the first-order, zone-center Raman active modes is

$$\Gamma_{Raman} = 10A_g + 5B_g \quad (1)$$

In Fig. 4a we show the unpolarised Raman spectrum at ambient conditions of the  $\beta$ -Ga<sub>2</sub>O<sub>3</sub> NC sample studied in this work. According to the mode assignments of Ref. [13], seven of the Raman peaks that show up in the spectrum correspond to  $A_g$  symmetry modes, while the rest of features correspond to phonons with  $B_g$  symmetry. Altogether, eleven out of the fifteen modes expected for  $\beta$ -Ga<sub>2</sub>O<sub>3</sub> are visible in the Raman spectrum of the sample studied in this work.

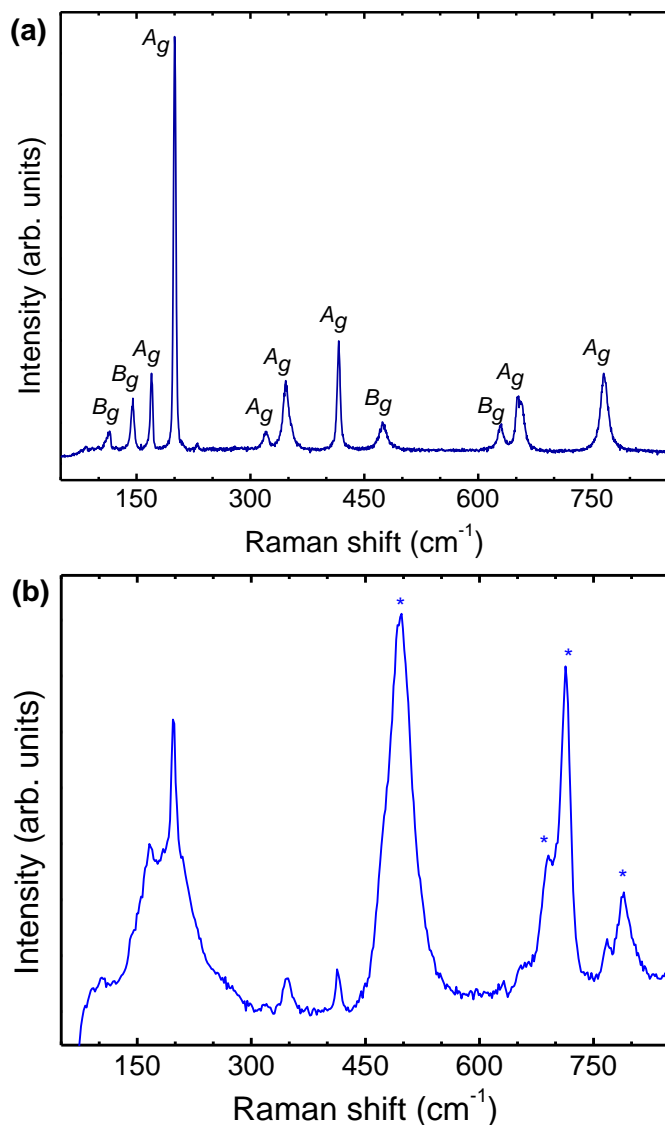


**Fig. 4.** Raman spectra for the  $\beta$ -Ga<sub>2</sub>O<sub>3</sub> sample outside the DAC (a) and inside the DAC at 0.47 GPa with silicone oil as pressure transmitting medium (b). Pointed peaks are attributed to the silicone oil scattering.

#### A. High-pressure Raman scattering of $\beta$ -Ga<sub>2</sub>O<sub>3</sub>

Once the  $\beta$ -Ga<sub>2</sub>O<sub>3</sub> was loaded into the DAC system with the silicone oil as pressure transmitting medium, high hydrostatic Raman scattering was studied from ambient pressure up to 21.63 GPa for the upstroke cycle in 25 steps, obtaining a total of fifteen peaks in this interval. From the comparison between the Raman scattering at high pressure (see Fig. 4b) and the previous experiment outside the anvil cell (Fig. 4a), it is deduced that there is a new source of scattering, since a new variety of peaks is observed. Actually, features appearing at ~496, ~696, ~713 and ~787 cm<sup>-1</sup> are attributed to the silicone oil. These features contribute to partially conceal the peaks corresponding to the  $\beta$ -Ga<sub>2</sub>O<sub>3</sub> NCs sample.

Figure 5 exhibits the Raman spectra of  $\beta$ -Ga<sub>2</sub>O<sub>3</sub> NCs at different hydrostatic pressures. As it can be seen, there is a clear shift of all the peaks (both  $\beta$ -Ga<sub>2</sub>O<sub>3</sub> and silicone) towards higher frequencies with increasing pressure. Indeed, at higher pressures, the interatomic distance decreases and consequently

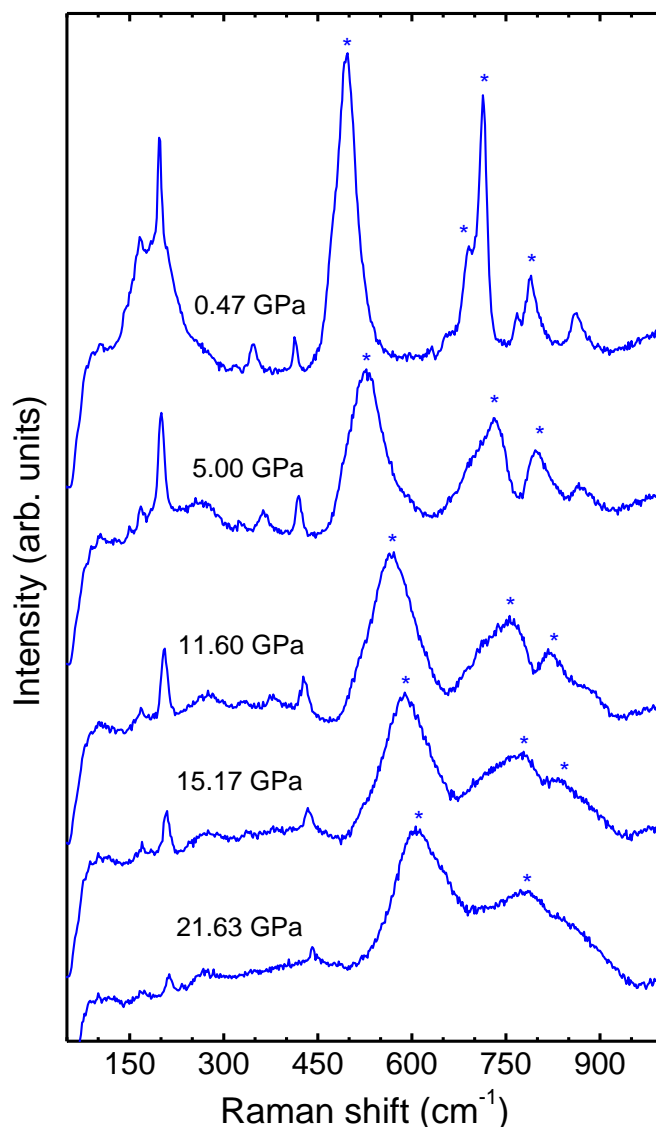


**Fig. 5.** Raman intensity under high-pressure as function of the position shift for some of the pressure values in the upstroke cycle. Peaks pointed with asterisks are attributed to the silicone oil scattering behaviour.

the spring constant of the phonon modes increases, leading to a blueshift of the Raman peaks.

In addition, the Raman peaks from the silicone oil present a more pronounced shift towards higher frequencies than those arising from  $\beta$ -Ga<sub>2</sub>O<sub>3</sub>, which reflects the larger compressibility of the silicone oil (<100 GPa in the pressure range considered in this work).

The dependence of the peak position as a function of applied pressure is shown in Fig. 6. There is a clear linear dependence of the frequency of the peaks as a function of the hydrostatic pressure in all the cases, although the difficulties in the observation of weaker peaks, partially due to the presence of the silicone oil features, do not allow us to monitor their pressure dependence along the whole pressure range. From a linear regression to the data of Fig. 6, the phonon pressure coefficients ( $d\omega/dP$ ) are extracted. Taking as  $\beta$ -Ga<sub>2</sub>O<sub>3</sub> NCs a bulk modulus of 202 GPa [13], Grüneisen parameters can be calculated.

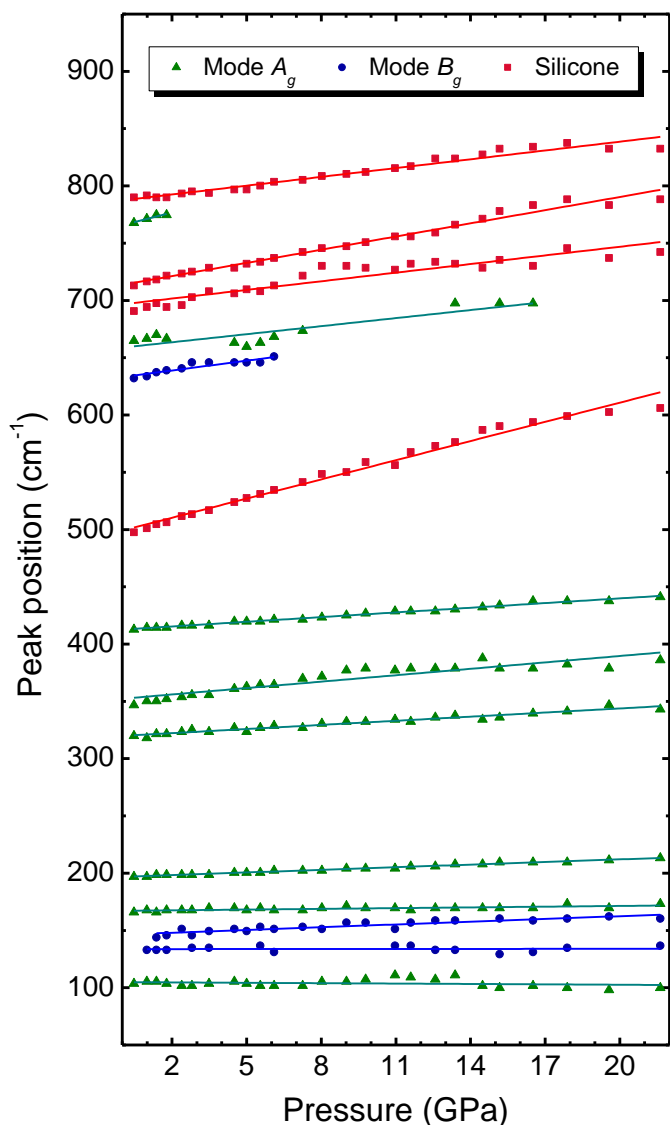


Fig. 6. Raman scattering peak position as a function of the applied pressure for the  $\beta$ -Ga<sub>2</sub>O<sub>3</sub> (with two symmetry modes,  $A_g$  and  $B_g$ ) with silicone oil as pressure transmitting medium in the cell.

The  $d\omega/dP$  values thus obtained for the different  $\beta$ -Ga<sub>2</sub>O<sub>3</sub> modes range from -0.11 to 5.54 cm<sup>-1</sup>/GPa. The magnitude of the different pressure coefficients partly reflects the different axial compressibilities of the monoclinic unit cell of  $\beta$ -Ga<sub>2</sub>O<sub>3</sub>. As reported in Ref. [13], the  $c$  axis is twice less compressible than the  $a$  axis, while the  $b$  axis has an intermediate compressibility. Thus, depending on the vibration direction of the Ga and O atoms for the different  $A_g$  or  $B_g$  modes, the phonon pressure coefficients may display sizably different pressure behaviours.

It is interesting to note that one of the modes with lower frequency shows a negative pressure coefficient, i.e., it is a soft mode. The observation of soft modes is usually linked to the presence of structural instabilities, which usually end up in first-order phase transitions. In the case of  $\beta$ -Ga<sub>2</sub>O<sub>3</sub>, a structural phase transition to the  $\alpha$  phase has been observed to occur at  $\sim$ 25 GPa in bulk samples [13]. In the present work, with applied pressure values lower than 22 GPa, no phase transition has been observed.

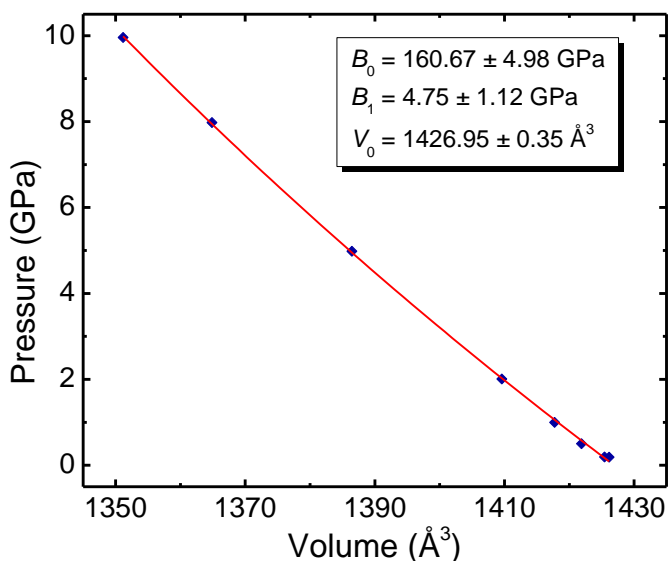


Fig. 7. Plot of calculated pressure as a function of the relaxed volume along with the fitted third-order Birch-Murnaghan equation of state. From the DFT calculations, a bulk modulus of  $B_0 = 160.7$  GPa is obtained.

The zero-pressure frequencies, phonon pressure coefficients and Grüneisen parameters obtained from the present Raman measurements are reported in Table I accordingly to the symmetry of the modes ( $A_g$  or  $B_g$ ). Available published data are also shown for comparison. As can be seen in the table, our experimental pressure coefficient values are slightly lower than those calculated and measured by Machon *et al.* [13]. This result is indicative of a lower compressibility in the case of the  $\beta$ -Ga<sub>2</sub>O<sub>3</sub> NCs studied in this work. This effect can be in principle attributed to the nanocrystalline nature of the material investigated in this work. To shed additional light on the origin of the lower compressibility of the NCs, next we present *ab initio* calculations of the structural properties of bulk  $\beta$ -Ga<sub>2</sub>O<sub>3</sub> as a function of pressure. Calculations of the vibrational properties of this compound are on the way.

### B. *Ab-initio* calculations

In order to confirm the experimental data of bulk [13] and  $\beta$ -Ga<sub>2</sub>O<sub>3</sub> NCs obtained with structural and vibrational techniques as a function of pressure, we have performed *ab initio* calculations for bulk material by using ground-state Kohn-Sham density functional theory (DFT). The aim of this study is to calculate the bulk modulus and compare it with the experimental value of 202 GPa reported by Machon *et al.* [13]. Note that, in that work, lattice dynamical DFT calculations as a function of pressure were performed. However, no structural data was given in that work. Thus, the present calculations are useful to confirm the validity of the experimental and theoretical results of Ref. [13] as well as an independent reference for the high-pressure Raman data obtained for the  $\beta$ -Ga<sub>2</sub>O<sub>3</sub> NCs.

The calculations were carried out by using the Quantum Espresso package [24] based on the Plane-Wave Self-Consistent Field (PWscf), which performs self-consistent calculations of electronic and structural properties using a plane-wave basis set [25]–[26]. The calculations were performed within the generalized gradient approximation

(GGA) by using the PBEsol functional, which is a revised Perdew-Burke-Ernzerhof GGA that is intended for solid state and surface systems [27]. Note that the lattice calculations of Ref. [13] were performed within the much simpler local density (LDA) approximation. For the calculations, a variable-cell relaxation was performed, using as initial coordinates for  $\beta$ -Ga<sub>2</sub>O<sub>3</sub> data obtained from the Crystallography Open Database (COD) and measured through the VESTA software [28]. Given that both Ga and O atoms occupy a 4i Wyckoff position in the unit-cell of  $\beta$ -Ga<sub>2</sub>O<sub>3</sub>, with  $y = 0$  or  $y = 1/2$  in all cases, only the  $x$  and  $z$  atomic coordinates were relaxed. The energy cutoff of the PW basis was chosen as 70 Rydberg, and the Brillouin zone integration for the total energy calculations was performed with a  $4 \times 6 \times 4$  grid.

With the aim of evaluate the bulk modulus as function of size, both final pressure and volume are determined for a set of pressures from 0 GPa up to 9.96 GPa. Then, the bulk modulus is obtained from the third-order Birch-Murnaghan equation of state,

$$P(V) = \frac{3B_0}{2} \left[ \left( \frac{V_0}{V} \right)^{\frac{7}{3}} - \left( \frac{V_0}{V} \right)^{\frac{5}{3}} \right] \left\{ 1 + \frac{3}{4} (B_0' - 4) \left[ \left( \frac{V_0}{V} \right)^{\frac{2}{3}} - 1 \right] \right\} \quad (2)$$

where  $V_0$  is the zero-pressure volume,  $B_0$  the bulk modulus at  $P = 0$  and  $B_0'$  the pressure derivative of the bulk modulus at  $P = 0$ . By fitting the theoretical  $P$ - $V$  curve with this expression,  $B_0$  is obtained (note that a narrower pressure interval than that employed during the high-pressure measurements was simulated).

Figure 7 shows the resulting points altogether with the third-order Birch-Murnaghan equation of state fitted. The resulting bulk modulus is equal to  $B_0 = 160.7 \pm 5.0$  GPa. This value is even lower than that measured with synchrotron XRD in Ref. [13] (202 GPa). The larger bulk modulus measured in Ref. [13] may partly be attributed to the fact that the XRD measurements reported in that work were done up to 18 GPa, where the material is expected to be less compressible. A way to validate this assumption could be to extend the calculations up to the same interval or to study the pressure scattering

behaviour at reduced pressures in more steps.

Overall, the present DFT results for bulk  $\beta$ -Ga<sub>2</sub>O<sub>3</sub> are consistent with the structural and vibrational data of Ref. [13] and, therefore, they cannot explain the pressure behaviour of the phonon modes of the  $\beta$ -Ga<sub>2</sub>O<sub>3</sub> NCs studied in this work. In other works, the lower phonon pressure coefficients measured in the NCs cannot be attributed to a possible lower compressibility for the bulk material than that reported experimentally and theoretically in Ref. [13]. As a consequence, the pressure dependence of the Raman modes in the NCs can be solely attributed to the nanocrystalline nature of the investigated sample.

#### IV. DISCUSSION

In order to explain the possible effect of the NCs on the compressibility of  $\beta$ -Ga<sub>2</sub>O<sub>3</sub>, several hypothesis are summarized, whose demonstration or disproof might be part of further investigations. Substrate effects, matrix-induced strain or particular size/morphology effects have been reported in the past as being responsible for increased/decreased compressibilities in nanostructured materials. For instance, Dubrovinskaia *et al.* [29] analysed the synthesis of aggregated diamond nanorods at 20 GPa; in spite of being this compound the densest carbon based material, it has yielded the lowest experimentally determined compressibility so far. Similarly, superhard aggregated boron nitride nanocomposites were studied [30]; the authors reported in this case a transition from a hardening (Hall-Petch effect) to a softening (inverse Hall-Petch effect) as function of the grain size, attributed to intergranular deformation by grain boundary sliding. Comparable phenomena were observed in other works about silicon nanowires [31]–[32], and in this case the reduced compressibility was attributed to the elastic behaviour induced by the very wire-like structure at the nanoscale. In other cases, the compressibility of epilayered material is found to strongly depend on the compressibility of the substrate, as is the case of InGaN thin films grown on sapphire or Si substrates [5].

Relative to the polymorphic transformation expected to occur at high pressures, in our experimental results there is not any first-order phase transition up to 21.63 GPa. However, the

TABLE I  
PHONON PRESSURE COEFFICIENTS AND GRÜNEISEN PARAMETERS

Mode symmetry	EXPERIMENTAL RESULTS [This work]			MEASURED RESULTS [13]		CALCULATED RESULTS [13]	
	$d\omega/dP$ (cm <sup>-1</sup> /GPa)	Frequency (cm <sup>-1</sup> )	Grüneisen parameter	Frequency (cm <sup>-1</sup> )	Grüneisen parameter	Frequency (cm <sup>-1</sup> )	Grüneisen parameter
$A_g$	-0.11	104.9	-0.22	110.2	-	104	1.39
$B_g$	0.013	133.7	0.019	113.6	-	113	-0.7
$B_g$	0.80	146.4	1.11	144.7	1.98	149	1.53
$A_g$	0.21	167.1	0.26	169.2	0.35	165	1
$A_g$	0.76	196.8	0.79	200.4	0.98	205	1.3
$A_g$	1.20	319.9	0.76	318.6	0.95	317	1.13
$A_g$	1.87	352.3	1.07	346.4	1.52	346	1.83
$A_g$	1.36	412.7	0.67	415.7	0.78	418	0.58
Silicone	5.49	496.6	2.24	-	-	-	-
$B_g$	2.85	633.2	0.91	628.7	1.54	626	0.8
$A_g$	2.34	658.8	0.72	652.5	1.39	637	1.39
Silicone	2.51	696.6	0.73	-	-	-	-
Silicone	3.84	713.6	1.09	-	-	-	-
$A_g$	5.54	765.7	1.47	763.9	1.11	732	1.23
Silicone	2.56	787.4	0.66	-	-	-	-

Calculated pressure coefficients and Grüneisen parameters for the upstroke cycle, compared with measured and calculated results by Machon *et al.* [13].

thermodynamics of phase transition within nanocrystalline samples are considerably altered compared with those for bulk materials [3]. Although it is verified that Ga<sub>2</sub>O<sub>3</sub> presents a transition phase from  $\beta$  to  $\alpha$ , there is still a controversy about the value of the pressure transition. In Ref. [13] it was reported a phase transition at 20-22 GPa; discrepancies were presented by Lipinska-Kalita *et al.* [14] with a beginning transition value much lower, at 6.5-7 GPa. Furthermore,  $\beta$ -Ga<sub>2</sub>O<sub>3</sub> nanocrystals were studied in other works [15], locating a transition from 13.6-16.4 GPa to 39.2 GPa. The transition phase was observed to begin at 6 GPa for nanocrystalline  $\beta$ -Ga<sub>2</sub>O<sub>3</sub> particles embedded in a glassy matrix [16], and the transition was not complete at 15 GPa, the highest value achieved in the study. Moreover, from this latter study, it can be concluded that the silica glass host matrix implied relevant structural and density changes within the pressure range. However, it is not yet known if these structural changes were intrinsic to nanocrystalline  $\beta$ -Ga<sub>2</sub>O<sub>3</sub> or promoted by anomalous densification among the silica matrix. In our case, it is not clear whether the silicone oil employed as pressure transmitting medium is affecting the compression behaviour of the NCs. Additional work using different pressure transmitting media would be necessary in order to ascertain this point.

A good strategy to associate the high-pressure induced behaviour of  $\beta$ -Ga<sub>2</sub>O<sub>3</sub> NCs with lattice parameters is to study the XRD at high pressures. In previous studies [17] about x-ray diffraction techniques in the DAC, it was reported a transformation from a  $\alpha$ -Ga<sub>2</sub>O<sub>3</sub> form to a tetragonal structure at 13.3 GPa; moreover, the x-ray diffraction pattern of the starting material strongly resembled a  $\beta$ -Ga<sub>2</sub>O<sub>3</sub> rather than  $\alpha$ -Ga<sub>2</sub>O<sub>3</sub>, with a mixture of phases present. Therefore, further XRD experiments at high pressures could be an alternative to study polymorphic transitions and to ascertain whether the present Raman results actually arise from the nanocrystalline nature of the samples investigated.

Given the contradictory results that can be found in the literature regarding the structural properties of  $\beta$ -Ga<sub>2</sub>O<sub>3</sub>, it is clear that more work is required. On the one hand, it would be necessary to investigate the high-pressure structural and vibrational properties of bulk and nanostructured  $\beta$ -Ga<sub>2</sub>O<sub>3</sub>, with the aim of fully understanding the origin of the lower compressibility displayed by the nanocrystalline  $\beta$ -Ga<sub>2</sub>O<sub>3</sub> sample studied here. On the other hand, since impurities could also distort the monoclinic lattice of  $\beta$ -Ga<sub>2</sub>O<sub>3</sub> and modify its structural properties and compression behaviour, it would also be necessary to compare experimental results from doped and undoped material. Note, for instance, that the results of Ref. [13] were obtained on annealed powder that originally contained 30% of the  $\alpha$  phase. It is likely that those samples contained a large amount of impurities, in contrast to the sample investigated in this work. Given that there are commercially available  $\beta$ -Ga<sub>2</sub>O<sub>3</sub> substrates grown with epitaxial techniques, it would be very interesting to perform such additional studies on this high-quality material.

## V. CONCLUSIONS

We have performed high-pressure Raman scattering measurements of monoclinic  $\beta$ -Ga<sub>2</sub>O<sub>3</sub> nanocrystals. Our experimental results have been complemented with structural *ab initio* calculations for the bulk material as a function of pressure.

SEM images (Fig. 1) and XRD spectra (Fig. 2) confirm the nanocrystalline nature of the  $\beta$ -Ga<sub>2</sub>O<sub>3</sub> sample here investigated. The Raman-scattering measurements at ambient pressure (Fig. 4a) show the typical  $\beta$ -Ga<sub>2</sub>O<sub>3</sub> scattering behaviour, without any anomalous active mode. Nevertheless, when high hydrostatic pressure is applied to the sample altogether with silicone oil as pressure transmitting medium, a new variety of peaks appears (Fig. 4b). These peaks are attributed to the silicone oil, some of which overlap with peaks of the  $\beta$ -Ga<sub>2</sub>O<sub>3</sub> NCs when pressure is increased.

Phonon pressure coefficients for the  $\beta$ -Ga<sub>2</sub>O<sub>3</sub> modes are determined within -0.11 and 5.54 cm<sup>-1</sup>/GPa, slightly below values reported in the literature for bulk samples. From the interpretation of the obtained Grüneisen parameters, it is possible to identify the symmetry modes  $A_g$  and  $B_g$  of  $\beta$ -Ga<sub>2</sub>O<sub>3</sub> NCs as well as the silicone oil modes. The difference between the present data and the results previously reported for bulk material can be attributed to the nanocrystalline nature of the samples here investigated.

To corroborate that bulk  $\beta$ -Ga<sub>2</sub>O<sub>3</sub> is more compressive than the nanocrystalline material, *ab initio* calculations have been performed. The resulting bulk modulus of  $160.7 \pm 5.0$  GPa confirms that bulk  $\beta$ -Ga<sub>2</sub>O<sub>3</sub> is more compressible than the NCs. Comparable results have been reported in the literature for different types of nanocrystalline samples.

No polymorphic transition for the  $\beta$ -Ga<sub>2</sub>O<sub>3</sub> has been observed up to 21.63 GPa, although there is not a clear pressure interval where the transition should take place. Besides, the transition processes for nanocrystalline samples strongly differ from those for bulk materials.

In summary, a hardening effect has been experimentally observed for the  $\beta$ -Ga<sub>2</sub>O<sub>3</sub> NC sample as a consequence of its nanocrystalline structure. More experimental is required in order to fully understand the origin of the lower compressibility displayed by the NCs studied in this work.

## ACKNOWLEDGMENT

My most sincere gratitude to both supervisors of this project, Dr. Jordi Ibáñez and Dr. Sergi Hernández, for their patience, support and advices and for giving me the opportunity of doing this work with them.

I would also like to mention the *nanocrew* I had the pleasure to meet during this Master: my thanks for all these months among you, and my best wishes for whatever comes into your future.

## REFERENCES

- [1] Long, D. A., & Long, D. A. (1977). *Raman spectroscopy* (Vol. 206). New York: McGraw-Hill.
- [2] Weber, W. H., & Merlin, R. (Eds.). (2013). *Raman scattering in materials science* (Vol. 42). Springer Science & Business Media.
- [3] Tolbert, S. H., & Alivisatos, A. P. (1995). High-pressure structural transformations in semiconductor nanocrystals. *Annual Review of Physical Chemistry*, 46(1), 595-626.
- [4] Ibanez, J., Hernández, S., López-Vidrier, J., Hiller, D., Gutsch, S., Zacharias, M., ... & Garrido, B. (2015). Optical emission from Si O 2-embedded silicon nanocrystals: A high-pressure Raman and photoluminescence study. *Physical Review B*, 92(3), 035432.
- [5] Oliva, R., Ibáñez, J., Cuscó, R., Dadgar, A., Krost, A., Gandhi, J., ... & Artús, L. (2014). High-pressure Raman scattering in InGaN heteroepitaxial layers: Effect of the substrate on the phonon pressure coefficients. *Applied Physics Letters*, 104(14), 142101.
- [6] Oliva, R., Ibanez, J., Artús, L., Cuscó, R., Zuniga-Perez, J., & Munoz-Sanjose, V. (2013). High-pressure Raman scattering of CdO thin films grown by metal-organic vapor phase epitaxy. *Journal of Applied Physics*, 113(5), 053514.
- [7] Ibáñez, J., Sans, J. A., Popescu, C., López-Vidrier, J., Elvira-Betanzos, J. J., Cuenca-Gotor, V. P., ... & Munoz, A. (2016). Structural, Vibrational, and Electronic Study of Sb<sub>2</sub>S<sub>3</sub> at High Pressure. *The Journal of Physical Chemistry C*, 120(19), 10547-10558.
- [8] Decremps, F., Pellicer-Porres, J., Saitta, A. M., Chervin, J. C., & Polian, A. (2002). High-pressure Raman spectroscopy study of wurtzite ZnO. *Physical Review B*, 65(9), 092101.
- [9] Proctor, J. E., Gregoryanz, E., Novoselov, K. S., Lotya, M., Coleman, J. N., & Halsall, M. P. (2009). High-pressure Raman spectroscopy of graphene. *Physical Review B*, 80(7), 073408.
- [10] Stepanov, S. I., Nikolaev, V. I., Bougrov, V. E., & Romanov, A. E. (2016). Gallium Oxide: Properties and Applications – A Review. *Rev. Adv. Mater. Sci*, 44, 63-86.
- [11] He, H., Blanco, M. A., & Pandey, R. (2006). Electronic and thermodynamic properties of β-Ga<sub>2</sub>O<sub>3</sub>. *Applied physics letters*, 88(26), 261904.
- [12] Nikolaev, V. I., Maslov, V., Stepanov, S. I., Pechnikov, A. I., Krymov, V., Nikitina, I. P., ... & Romanov, A. E. (2017). Growth and characterization of β-Ga<sub>2</sub>O<sub>3</sub> crystals. *Journal of Crystal Growth*, 457, 132-136.
- [13] Machon, D., McMillan, P. F., Xu, B., & Dong, J. (2006). High-pressure study of the β-to-α transition in Ga<sub>2</sub>O<sub>3</sub>. *Physical Review B*, 73(9), 094125.
- [14] Lipinska-Kalita, K. E., Kalita, P. E., Hemmers, O. A., & Hartmann, T. (2008). Equation of state of gallium oxide to 70 GPa: Comparison of quasihydrostatic and nonhydrostatic compression. *Physical Review B*, 77(9), 094123.
- [15] Wang, H., He, Y., Chen, W., Zeng, Y. W., Stahl, K., Kikegawa, T., & Jiang, J. Z. (2010). High-pressure behavior of β-Ga<sub>2</sub>O<sub>3</sub> nanocrystals. *Journal of Applied Physics*, 107(3), 033520.
- [16] Lipinska-Kalita, K. E., Chen, B., Kruger, M. B., Ohki, Y., Murowchick, J., & Gogol, E. P. (2003). High-pressure x-ray diffraction studies of the nanostructured transparent vitroceraic medium K<sub>2</sub>O–SiO<sub>2</sub>–Ga<sub>2</sub>O<sub>3</sub>. *Physical Review B*, 68(3), 035209.
- [17] Tu, B., Cui, Q., Xu, P., Wang, X., Gao, W., Wang, C., ... & Zou, G. (2002). The pressure-induced phase transition of Ga<sub>2</sub>O<sub>3</sub>. *Journal of Physics: Condensed Matter*, 14(44), 10627.
- [18] Young, R. A. (1993). *The rietveld method* (Vol. 5, pp. 1-38). International union of crystallography.
- [19] Lopez, I., Utrilla, A. D., Nogales, E., Mendez, B., Piqueras, J., Peche, A., ... & González-Calbet, J. M. (2012). In-doped gallium oxide micro- and nanostructures: morphology, structure, and luminescence properties. *The Journal of Physical Chemistry C*, 116(6), 3935-3943.
- [20] Wang, G., Park, J., Kong, X., Wilson, P. R., Chen, Z., & Ahn, J. H. (2008). Facile Synthesis and Characterization of Gallium Oxide (β-Ga<sub>2</sub>O<sub>3</sub>) 1D Nanostructures: Nanowires, Nanoribbons, and Nanosheets. *Crystal Growth and Design*, 8(6), 1940-1944.
- [21] Letoullec, R., Pinceaux, J. P., & Loubeyre, P. (1988). The membrane diamond anvil cell: a new device for generating continuous pressure and temperature variations. *International Journal of High Pressure Research*, 1(1), 77-90.
- [22] Oliva Vidal, R. (2016). High-pressure optical and vibrational properties of InN and InGaN.
- [23] Mao, H. K., Bell, P. M., Shaner, J. T., & Steinberg, D. J. (1978). Specific volume measurements of Cu, Mo, Pd, and Ag and calibration of the ruby R 1 fluorescence pressure gauge from 0.06 to 1 Mbar. *Journal of applied physics*, 49(6), 3276-3283.
- [24] Giannozzi, P., Baroni, S., Bonini, N., Calandra, M., Car, R., Cavazzoni, C., ... & Dal Corso, A. (2009). QUANTUM ESPRESSO: a modular and open-source software project for quantum simulations of materials. *Journal of physics: Condensed matter*, 21(39), 395502.
- [25] Payne, M. C., Teter, M. P., Allan, D. C., Arias, T. A., & Joannopoulos, J. D. (1992). Iterative minimization techniques for ab initio total-energy calculations: molecular dynamics and conjugate gradients. *Reviews of Modern Physics*, 64(4), 1045.
- [26] Jones, R. O. (2015). Density functional theory: Its origins, rise to prominence, and future. *Reviews of modern physics*, 87(3), 897.
- [27] Perdew, J. P., Ernzerhof, M., & Burke, K. (1996). Rationale for mixing exact exchange with density functional approximations. *The Journal of Chemical Physics*, 105(22), 9982-9985.
- [28] Momma, K., & Izumi, F. (2011). VESTA 3 for three-dimensional visualization of crystal, volumetric and morphology data. *Journal of Applied Crystallography*, 44(6), 1272-1276.
- [29] Dubrovinskaia, N., Dubrovinsky, L., Crichton, W., Langenhorst, F., & Richter, A. (2005). Aggregated diamond nanorods, the densest and least compressible form of carbon. *Applied Physics Letters*, 87(8), 083106.
- [30] Dubrovinskaia, N., Solozhenko, V. L., Miyajima, N., Dmitriev, V., Kurakevych, O. O., & Dubrovinsky, L. (2007). Superhard nanocomposite of dense polymorphs of boron nitride: Noncarbon material has reached diamond hardness. *Applied Physics Letters*, 90(10), 101912.
- [31] Khachadorian, S., Papagelis, K., Scheel, H., Colli, A., Ferrari, A. C., & Thomsen, C. (2011). High pressure Raman scattering of silicon nanowires. *Nanotechnology*, 22(19), 195707.
- [32] Wang, Y., Zhang, J., Wu, J., Coffey, J. L., Lin, Z., Sinogeikin, S. V., ... & Zhao, Y. (2008). Phase transition and compressibility in silicon nanowires. *Nano letters*, 8(9), 2891-2895.